

Military Technical College  
Kobry Elkobba,  
Cairo, Egypt



8<sup>th</sup> International Conference  
on Aerospace Sciences &  
Aviation Technology

**NUCLEATE POOL BOILING FROM PLAIN AND ENHANCED SINGLE TUBE TO R12 AND R134a FOR AIR-CONDITIONING EVAPORATORS**

Mohammed A. Aziz\*, Sayed A. Sayed\*\*, I. Aly Gad\*\*\* and A. El Refai\*\*\*\*  
Department of Mechanical Power Engineering  
Faculty of Engineering, Zagazig University  
Zagazig, Egypt.

**ABSTRACT**

Measurements of pool boiling heat transfer coefficients in pure R12 and R134a are reported for a plain tube (PT) and three enhanced tubes: (Screen Matrix tube, (SM) and two integral finned tubes: Radial (RF) and longitudinal LF). The data were taken at saturation temperatures of -5, and 5 °C, and heat flux range from  $2 \times 10^3$  to  $10^4$  W/m<sup>2</sup>. All enhanced tubes provide higher boiling coefficients than the plain tube does. The slopes of the boiling coefficient vs the heat flux curves for enhanced tubes are smaller than those for the plain tube, indicating the dominating effect of enhanced surfaces conditions. The mechanism describing the generation, growth and separation of bubbles for tested enhanced tubes was elaborated. The highest boiling coefficient was found to belong to the screen matrix tube, having the highest nucleation sites density. Additional achievement was observed when R134a was tested at the considered operating condition. Two correlations for predicting the boiling coefficients from the present considered surfaces were developed with satisfactory accuracy for the design of refrigerant flooded evaporators.

**Key Words :** Pool Boiling, R12, R134a, Enhanced Surface.

**NOMENCLATURE**

A	heat transfer area, [m <sup>2</sup> ]	$\theta$	contact angle, [deg]
$C_p$	isobaric specific heat, [J/kg.K]	$\rho$	density [kg/m <sup>3</sup> ],
D	tube diameter [m]	$\sigma$	surface tension, [N/m]
$d_f$	Fritz bubble departure diameter[m].	[m]	$\alpha$ boiling coefficient, (W/m <sup>2</sup> K)
$d_o$	modified bubble departure diameter) [m]	$\psi$	constant, (Eq 15)
g	acceleration due to gravity, [m.s <sup>-2</sup> ]	$\phi$	void fraction, (Eq. 11)
$h_{fg}$	latent heat of vaporization, [J/kg]	$\gamma$	exponent (Eq.12)
$K_p$	Kutatekadze boiling number	$\delta_f$	liquid film thickness [m]
k	thermal conductivity, [W/m K]	<b>Subscripts</b>	
L	length, [m]	cr	critical
M	molecular weight, [kg/kmol]	en	enhanced
m	exponent	f	film
N	nucleation sites density, [m <sup>-2</sup> ]	l	liquid
Nu	Nusselt number	min	minimum
n	exponent	p	plain
Pr	Prandtl number	$P_o$	pore
P	pressure, [k Pa]	s	saturation
q	heat flux, [W/m <sup>2</sup> ]	sv	saturation vapor
Re	Reynolds Number	v	vapor
r	bubble radius, [m]	w	wall
T	temperature, [K]		
t	temperature (°C)		
x	reference length [m]		

\* Assoc. Prof. Dpt. of Mech. Power Zagazig University, Zagazig Egypt

\*\* Prof. Dpt. Of Mech. Power Zagazig University, Zagazig Egypt

\*\*\* Lect. Dpt. Of Mech. Power Zagazig University, Zagazig Egypt

## INTRODUCTION

In the air conditioning and refrigeration industries flooded evaporators are used where a refrigerant boils on the outside of a tube bundle, whereby it cools the chilled water circulating through the tubes. It is postulated that the heat transfer coefficient of boiling refrigerant is rather lower than that of circulating water. This statement necessitates the need to find ways to improve the heat transfer of boiling refrigerant, in order to design more compact and efficient evaporators, as reported by Choomac and Aziz [1]. The influence of surface condition on boiling heat transfer has been proven to be dominant. These surfaces can take a number of enhancement forms such as ; (1) roughening surface generated by lapping, or sanding proving an increased number of nucleation sites, (2) mechanical working in the form of low integral fins / radial or longitudinal with varying fin profile and (3) covering the surface by porous coatings composed of nearly spherical particles or by lagging the surface by fine screen matrix.

The enhancement of these surfaces serves to increase vapor gas entrapment volume and active nucleation sites density. These increases combine to reduce incipient superheat and nucleate boiling superheat ( $T_w - T_s$ ) and hence, increases the boiling heat transfer coefficient. In recent years, significant progress has been made toward the understanding of nucleate boiling heat transfer; and correlations have been developed in order to precisely design flooded evaporators.

At the present time; the refrigeration industries are undergoing a massive conversion process from CFCs, to HFCs. This conversion established a need for the data on replacement refrigerants such R134a used instead of R12. In this concern, few works have been done with regard to nucleate boiling and are summarized by Pais and Webb [2].

Only some of relevant studies are reviewed here. Pool boiling of R22, R124 and R134a on plain tube was studied by Chou and Lu [3] at saturation temperatures of 4.4 and 26.5 °C. Numerous data exist on pool boiling heat transfer from rib-roughened and low-integral finned surfaces for a wide variety of refrigerants are given in refs. [4 through 7]. Recently, porous metallic coatings, as an enhancement technique has received a great interest by many researchers. In this concern, Chang and You [8 and 9] examined the effect of coating composition from micro-porous surfaces on boiling heat transfer phenomena. Aziz [10] studied experimentally the nucleate boiling of R22 on a single tube with various screen matrix geometries (as a form of porous coating). Later, Hsieh and Weng [11] reported results of an experimental study on nucleate pool boiling from coated surfaces in saturated R134a and R-407c.

From the above-given review, it is noticed that a considerable amount of published data exists in literature on nucleate boiling enhancement. However, few studies have been devoted to highlight the effects of surface enhancement on heat transfer coefficient of boiling refrigerants. Besides, the published data of nucleate boiling are not consistent with each other, as reported by Stephan and Abdel - Salam [13]. As such, it is difficult to predict the heat transfer coefficient with satisfactory accuracy, specially for the new refrigerant R134a, boiling on enhanced surfaces. Thus, the objective of this paper is to enrich the pool boiling data base for zero ozone depletion refrigerant R134a as an alternative to R12, by providing heat transfer experimental data from a variety of enhanced surfaces. Also to develop correlations suitable for present enhanced surfaces, which help to predict heat transfer coefficient of boiling R12 and R134a for flooded evaporator in air-conditioning applications.

## EXPERIMENTS

### Test Facility

The schematic of the single-tube pool boiling apparatus is shown in Figure 1. It consists of two closed loops: (1) the test section of R12 or R134a boiling loop and (2) R12 cooling loop. The pool boiling loop consists of a cylindrical test vessel (evaporator), condenser, and relevant connecting copper pipes. The evaporator and condenser are arranged to provide reflux operation. The evaporator containing the tested tube immersed in the tested refrigerant, is located beneath the reflux condenser. The generated vapor leaves the test section through the vapor line to the reflux condenser. The condensate falls back to the evaporator by gravity. The reflux condenser is cooled by R12 flowing through the cooling loop evaporator which is arranged inside it. Thus, the pressure inside the test loop was controlled by varying the rate at which R12 was passed through the cooling loop evaporator.

The test cylindrical vessel (evaporator), is made of copper with diameter of 170 mm and length of 230 mm. The test vessel has two lateral windows to observe the boiling phenomenon. The vessel was also provided with ports for electric wires, pressure gauges, and thermocouple leads. The test tube was (fabricated from a copper rod) designed to simulate a portion of typical rod in refrigerant-flooded type evaporator. The copper rod was 25 mm in outer diameter, and of total length of 140mm.

The evaporator tube was heated by means of a 500 Watt nickel - chromic heater, covered with ceramic rings to insulate the heater from the tube wall. The heater with ceramic rings was inserted into a cavity that axially drilled through the shank, as shown in Figure 2.

To minimize longitudinal heat conduction, devcon epoxy glue mixed with silicon powder were applied at the ends of the tube. Four copper-constantan thermocouples were installed in the wall of the copper rod, for temperature measurements at four circumferential positions. Each tested tube was positioned accurately inside the vessel - evaporator by means of Teflon bushings. These bushings fitted into two vertical Perspex plates.

In present work three various enhanced tubes (Radial Integral finned (RF), longitudinal Integral Finned (LF) tubes and tube covered by a single layer of screen matrix (SM) have been examined and compared with plain tube (PT). The geometries of the tested tubes are illustrated in Figure 2.

**Measurements**

Tested tube wall temperature was measured using four calibrated copper - constantan shielded thermocouples. The liquid temperature in the vessel - evaporator was measured by means of two thermocouple placed close to the liquid free surface and were fixed to the tubes frame plate. The temperature readings were taken off by a type. Sense-Digi thermometer accurate to within  $\pm 0.1$  °C of measured values.

A pressure gauge calibrated to an accuracy of  $\pm 0.5$  % of the indicated reading, is placed at the top of vessel - evaporator to measure the pressure inside it. For this purpose , two pressure gauges for R12 and R134a were used.

The electric power applied to the tube heater was directly measured using a digital BRI - 5040 type wattmeter having an accuracy of  $\pm 1$ % of the indicated readings.

**Experimental procedure**

Prior to undertaking the test run, the vessel evaporator and tested tube were cleaned with acetone before charging with tested refrigerant. Once, the tested tube was installed, the system was evacuated by a vacuum pump to an absolute pressure of  $\approx 3$  kPa. With no leak detected over a period of 24 h, the evaporator vessel was charged with pure refrigerant (gas) from a commercial reservoir to a level of 30 mm above the top of the tested tube.

Before the experiments were performed , the test tube was heated with the highest heating rate of  $q = 10$  kW/m<sup>2</sup> for at least 20 h in order to avoid the starting effects until the heat transfer coefficient reached approximately a constant value. The temperature of liquid refrigerant was adjusted to the predetermined value by varying the flow rate of R12 circulating through the cooling loop. For all tested tubes, the heat flux was first set at a maximum value of 10 kW/m<sup>2</sup> until steady state condition is attained. The criterion of steady state condition was the constancy of the saturation and wall surface temperatures over a period of 10 min. To achieve these conditions, necessary adjustment were made for the supplied power to the heater and cooling refrigerant flow rate. Once, the heat flux has been fixed and the required saturation temperature in the pool was maintained, several readings were taken of the tube wall temperature, power supply, and saturation temperature of the tested refrigerant. The recorded values were averaged. Data collection was then commenced with decreasing heat flux in predetermined steps down to around 2 kW/m<sup>2</sup>.

**Data Reduction**

The heat transfer coefficient ( $\alpha$ ), for each value of power input was calculated as follows:

$$\alpha = \frac{Q}{A \cdot (T_w - T_s)} \tag{1}$$

Where Q is the electric power supplied to the heater, T<sub>s</sub> and T<sub>w</sub> , are the saturation and average wall temperatures, respectively.

A<sub>e</sub> is the effective outer surface area based on smooth tube and evaluated as  $\pi DL$ , where D is the envelope diameter of tested tube as recommended by [5,10,12] , and L is the effective tube length.

The average outer wall temperature, T<sub>w</sub> , is given by.

$$T_w = \sum_{n=1}^{n=4} T_{wi} / 4 \tag{2}$$

**THEORY**

In nucleate boiling, bubbles are created by expansion of entrapped gas or vapor in small cavities in the surface. The bubbles grow to a certain size, depending on the temperature, pressure and the surface tension at the liquid - vapor interface. These bubbles, depending on the temperature excess may collapse, may expand and

detach from the surface to dissipate in the liquid. Considering a bubble of spherical form, the pressure forces of the liquid and vapor must be balanced by surface tension force at vapor-liquid interface, that is :

$$\pi r^2(P_v - P_l) = 2 \pi r \sigma \tag{3}$$

or 
$$\Delta P = P_v - P_l = \frac{2\sigma}{r} \tag{4}$$

For small value of pressure difference .  $\Delta P$  can be approximated to 
$$\Delta P \approx \Delta T(\partial P / \partial T)_s \tag{5}$$

where 
$$\Delta T = T_{s,v} - T_s \tag{6}$$

In Equation (6)  $T_{s,v}$ ; and  $T_s$  are the saturation temperatures of vapor and liquid phases, respectively. As the bubbles are created at surface cavities,  $T_{s,v}$  can therefore be approximated to  $T_w$ .

The derivative of pressure with respect to temperature at saturation line  $(\partial P/\partial T)_s$ , is expressed in accordance with Clapeyron - Clausius law as:

$$(\partial P / \partial T)_s = \frac{h_{fg} \cdot \rho_v \cdot \rho_l}{T_s(\rho_l - \rho_v)} \tag{7}$$

Inserting equations (5) and (7) into Eq (4), and considering that  $\rho_v \ll \rho_l$  we have an expression for the (critical) radius of bubbles, which corresponds to the size of nucleation site, that is :

$$r_{cr} = \frac{2\sigma T_s}{\Delta T \cdot h_{fg} \rho_v} \tag{8}$$

The vapor bubble generated on the wall grows to a certain size, characterized by the diameter, at which it separates from the wall. Fritz, theoretically calculated the volumes of vapor bubbles before separation from the surface under static condition and for various contact angles. The departure diameter is given by

$$d_f = 0.0208 \theta \sqrt{\sigma / g(\rho_l - \rho_v)} \tag{9}$$

where  $\theta$ , is the contact angle. For liquid refrigerants contact angle  $\theta = 60$  degrees.

Properties of liquid are to be evaluated at the saturation temperature  $T_s$ , whereas properties of vapor are to be evaluated at the film temperature,  $T_f$ , defined by,

$$T_f = (T_w + T_s) / 2 \tag{10}$$

## RESULTS AND DISCUSSIONS

All experiments were conducted for pool boiling of pure R12 and R134a at saturation temperatures of -5 and 5°C.

### Pool Boiling of Plain Tube

The plain tube was tested first. Figure 3 a-b, shows the boiling coefficient ( $\alpha$ ) vs heat flux ( $q$ ) at saturation temperatures of -5 and 5°C. The data were very repeatable and agree closely with those of Webb and Pais [5] for boiling R12, and R134a at saturation temperature of 4.4. °C. The good agreement of compared data confirms the present experimental measurements accuracy and the experimental procedure validity.

### Pool Boiling of Enhanced Tubes

In Figures 4 and 5 nucleate boiling performance characteristics (heat-transfer coefficient ( $\alpha$ ) vs the heat flux ( $q$ ) of enhanced tubes are compared for heat fluxes below 10 kW/m<sup>2</sup>. For comparison, nucleate boiling data for plain tube were also plotted. A similar trend of ( $\alpha$ ) vs ( $q$ ) is observed for all tubes. The global inspection of Figs 4a-b and 5a,b, shows that, the boiling coefficient increases with saturation temperature (or pressure) and heat flux. This is because, the increase of each or both contributes to increase the active nucleation sites number, resulting large heat transfer coefficients. Examination of all data sets shows that the slope of the  $\alpha$  vs  $q$ , curve is not equal for the various tubes. The plain tube exhibits the greatest slope (0.65 - 0.67) compared to those for enhanced tubes. The screen matrix tube has the lowest slope value (0.42-0.55). These different slopes evidently show the difference in nucleate boiling characteristics between the compared tubes.



**Performance Comparison of the Participating Tubes**

In general, enhanced tubes perform better than plain tube under all conditions, providing an enhancement ratio  $\alpha_e/\alpha_p$  of up to 1.1 ~ 2.9 times for RF tube, 3~4.6, for LF tube and 2.8 ~ 5 for SM tube. These ratios are also noticed to decrease with increasing heat flux demonstrating the significant effect of the surface conditions at relatively small heat fluxes, specified for refrigerant evaporators. Table (1) shows the enhancement ratio  $\alpha_e/\alpha_p$  for enhanced tubes.

Table 1: Enhancement ratio for enhanced tubes (The tabled ratios are determined from the data points).

Heat flux, W/m <sup>2</sup>	$\alpha_e / \alpha_p$											
	q = 2000				q = 5000				q = 9000			
	5		-5		5		-5		5		-5	
t <sub>o</sub> , C°	R12	R134	R12	R134	R12	R134	R12	R134	R12	R134	R12	R134
Refrigerant												
RF tube	1,3	2,4	1,4	2,9	1,2	2,3	1,3	2,8	1,1	2,1	1,2	2,5
LF tube	3,1	3,2	4,6	4,4	3,4	3,0	4,5	3,7	3,3	2,6	4,3	3,1
SM tube	3,4	3,4	5,0	4,7	3,2	3,3	4,8	4,1	3,5	2,8	4,7	3,3

The boiling coefficient enhancement on enhanced surface can in general be attributed to the good conditions of the formation, growth and separation of the bubble. The mechanism describing these stages is different for various surfaces as pointed by Afgan [14] and Zeigarnik [15].

The mechanism of bubble formation on plain tube is described in detail in refs. [16 through 18] and can be briefly described as follows: due to the heat supplied through the heated plain surface, vapor is generated in cavities Fig 6.I.a. Because of the pressure inside bubble P<sub>v</sub> is greater than liquid pressure P<sub>l</sub>, the bubble grows and expands to a certain size, shifting the liquid micro-layer toward the bulk of saturated liquid, Figure 6.1 b and c. When the bubble size reaches the departure diameter, d<sub>p</sub>, it separates from the heated surface and moves into a region whose temperature is below that of vapor. As a result, heat will be conducted out and bubble will collapse. Consequently, the heated liquid intake into cavities occurs and the process is then repeated. Figure 6.I.d. It is worth-noting that, during the boiling onset, the separation of bubbles from the superheated boundary layer into relatively colder fluid is considerably impeded. Accordingly, the activation of nucleation centers for subsequent bubble formation is only possible with larger superheat Δt (or greater heat flux, q and in the presence of relatively thick superheated liquid boundary layer. This is why plain surface exhibits poor boiling coefficient.

Concerning finned surfaces, the bubble formation mainly occurs in the fin base on the contact points with the tube surface Figure 6.II.a, the channels created by V shaped fins Fig 6.II.b, tend to impose bubble to slide around the channel in close contact with the tube. This provides a thin liquid micro-layer between the surface and bubble over a larger proportion of the heated surface. For this liquid micro-layer a low heat flux (q) or relatively small degree of superheat (Δt) is needed to nucleate it resulting a larger boiling coefficient compared with plain surface.

As reported by Aziz [10], screen matrix coating can be assumed as space with numerous meshes with homogeneous orientation in the form of open structure pores, interconnected throughout the porous coating, Fig 6.III.a. Evaporation of liquid layer existing in pores occurs intensively. This is due to the uniformly supplied heat flux through the tube wall and matrix coating, facilitating the formation of bubble, Fig 6.III.b. This can actually occur if the liquid layer thickness δ<sub>f</sub>, that separates bubble from wall is small. For porous coating δ<sub>f</sub> can be calculated according to Zeigarnik [15] as:

$$\delta_f = (1 - \varphi) d_{p_0} / 4 \tag{11}$$

Where d<sub>p<sub>0</sub></sub> is the pore diameter, and φ is the void fraction. In this study, d<sub>p<sub>0</sub></sub> is equal to 70 μm, whereas φ is ranging from 0.2 to 0.8. Considering φ = 0.8, the liquid film thickness is equal to 3.5 μm and the thermal resistance of the film constitutes (3.64 to 4.6) 10<sup>-5</sup> m<sup>2</sup>K/W. Bubble embryos protrudes from the pore when the vapor pressure becomes greater than liquid pressure. During the bubble growth period, vapor passes through the pores, the bubble radius increases and the bubble departs from the pore surface; leaving a part of vapor which will serve as a new bubble generation, Fig 6.III.d. So, the frequency of bubble formation on porous surface is expected to be smaller than other surfaces. As the bubble departs, intensive condensation takes place on the spherical bubble surface, releasing its latent heat to the colder liquid. Meanwhile the active nucleation site in fact functions as a micro heat pipe, for which the heated section is formed by the pore matrix. and the cooled section is adjacent to the colder liquid. As a result of bubble departure, the pressure in a pore becomes lower than for the

liquid pool. Due to the capillary forces acting inside the pore a thin film liquid intake occurs into pore to warrant the wetting of the heated surface.

To provide theoretical background, the calculated bubble size  $r_{cr}$ , incorporated with measured superheat,  $\Delta t$ , under certain conditions ( $t_s = 5^\circ\text{C}$  and  $q = 5000 \text{ Wm}^{-2}$ ) are listed in table 2.

Table 2. Bubble size ( $r_{cr}$ ) and degree of superheat ( $\Delta t$ ).

Tube	R12		R134a	
	$r_{cr}$ , (m)	$\Delta t$ , $^\circ\text{C}$	$r_{cr}$ , (m)	$\Delta t$ , $^\circ\text{C}$
PT	$4.8 \cdot 10^{-7}$	4.03	$6.4 \cdot 10^{-7}$	2.7
RF	$6.2 \cdot 10^{-6}$	3.2	$1.6 \cdot 10^{-6}$	1.15
LF	$1.9 \cdot 10^{-6}$	1.1	$2.0 \cdot 10^{-6}$	1.08
SM	$2.2 \cdot 10^{-6}$	1.05	$2.2 \cdot 10^{-6}$	0.8

An inspection of table (2) indicates that, Equation (8) describes the dimensions of nucleation sites for porous surface rather than for completed surfaces. This is due to larger nucleation site size  $r_{cr}$ , intensive boiling on pores due to the small resistance of liquid film, with much lower degree of superheat and significant ability of porous coating to trap vapor.

### Performance Comparison of the Competing Refrigerants

It is intended that R134a replaces R12, so, it is interesting to compare the boiling coefficient of R134a with that of R12. Test results for all tested tubes at saturation temperatures of 5 and  $-5^\circ\text{C}$  in Figures 4 and 5, indicate that the boiling coefficients for R134a are apparently higher than for R12. The main reason can be attributed to the physical properties of tested refrigerants illustrated in table (3). for prescribed saturation temperatures of  $-5$  and  $5^\circ\text{C}$ .

Table 3: Thermodynamic and Transport Properties of R12 and R134a Evaluated at  $T_s = 5$  and  $-5^\circ\text{C}$ . [22]

Fluid	$t_s$ , $^\circ\text{C}$	$h_{fg}$ , kJ/kg	$k_l$ , W/mK	$\mu_l$ , Pa.s	$\mu_v$ , Pa.s	$c_{pl}$ , J/kgK	$\rho_l$ , kg/m <sup>3</sup>	$\rho_v$ , kg/m <sup>3</sup>	$\sigma$ , N/m	Pr
R12	5	148.82	0.0746	$2.32 \cdot 10^{-4}$	$12.63 \cdot 10^{-6}$	972	1379	20.95	0.0117	3.022
	-5	154.52	0.07791	$2.61 \cdot 10^{-4}$	$12.18 \cdot 10^{-6}$	937	1412	15.33	0.0131	3.14
R134a	5	197.9	0.0912	$2.69 \cdot 10^{-4}$	$11.18 \cdot 10^{-6}$	1343	1276	1704	0.011	3.96
	-5	202.3	0.0958	$3.06 \cdot 10^{-4}$	$10.7 \cdot 10^{-6}$	1297	1308	1203	0.0124	4.14

The thermodynamic and transport properties for R134a ( $h_{fg}$ ,  $k_l$ , Pr and  $c_{per}$ ) are apparently higher than for R12 while  $\rho_v$  and  $\sigma$  for R134a are lower than corresponding values for R12. Consequently, the boiling coefficient of R134a are expected to be higher than those of R12. Table (4) provides the R134a to R12 boiling coefficient ratios for tested tubes under similar conditions.

Table 4: R134a to R12 boiling coefficient ratios for various tested tubes

Heat flux, $\text{W/m}^2$	$\alpha_{R134a} / \alpha_{R12}$					
	$q = 2000$		$q = 5000$		9000	
	5	-5	5	-5	5	-5
$t_o$ , $^\circ\text{C}$						
Plain tube	1.42	1.59	1.51	1.44	1.32	1.54
RF. Tube	3.13	2.60	2.83	4.06	2.31	2.78
LF. Tube	1.56	1.19	1.32	1.19	1.04	1.07
S.M. tube	1.6	1.11	1.39	1.23	1.04	1.04

From table (4) it is obvious that the lowest values of the ratio  $\alpha_{R134a} / \alpha_{R12}$  are belonging to the screen matrix tube. This can be attributed to the dominant effect of the surface conditions over the thermo-physical properties. However, it should be noted that the behaviour of these ratios may vary due to the variations of the thermo-physical properties of tested fluids, depending on the temperature range of conducted experiments.

**The Number of Nucleation Sites**

The nucleation sites number is one of the most important parameter affecting the boiling heat transfer coefficient. In 1966 Danilova [18] indicated that the surface roughness had a profound effect on the position and slope of the nucleate boiling. Later it was confirmed that, cavities and scratches were in fact nucleation sites. It has been generally agreed [2,19,20,21], that pool boiling active nucleation sites number N can be determined as a function of the cavity radius ( $r_{min}$ ) in the form :

$$N = C (r_{\alpha})^{\gamma} \tag{12}$$

In Equation (12), C and  $\gamma$  are constants characterizing the boiling surface. Unfortunately, Eq (12) can not be applied for practical purposes because of the deficiency of constants C and exponent  $\gamma$  values for new surface. However, based on the experimental data accumulated from a wide variety of sources, Ogulari and Ishi [19], proposed the following expression for the nucleation sites number, N as,

$$\frac{\alpha}{k_l} = 14 \left( \frac{\rho_l \cdot c_{pl} \cdot \Delta T}{h_{fg} \cdot \rho_v} \right)^{0.5} \cdot Pr^{-0.39} \cdot N^{-0.375} \cdot d_o^{-0.25} \tag{13}$$

where  $d_o$  is modified bubble departure diameter and is given by :

$$d_o = 0.0012 [\rho_l - \rho_v] / \rho_v^{0.9} \cdot d_f \tag{14}$$

$d_f$ , is the Fritz bubble departure diameter, which is determined from Eq. (9). Considering the variety of the surfaces and fluids used in the present experiments, the nucleation sites density N predicted from Eq. (13) for the whole experimental range is presented in Fig. 7 as a function of the thermo-physical properties and experimental parameters. From this figure it is evident that, enhanced surfaces generally exhibit greater nucleation site density than does the plain surface. In addition, the greatest value of N is belonging to the screen matrix surface. This confirms the present suggestion on the mechanism of nucleation, growing, and separation of bubbles from the tested surfaces.

**Correlation**

There are a number of correlation's available in literature to predict the pool boiling heat transfer coefficient for a plain and enhanced tubes in pure liquid. The most of these can be reduced to a common form expressing heat transfer coefficient as a function of heat flux and pressure:

$$\alpha = \psi_1 q^{n_1} \cdot P^{m_1} \tag{15}$$

where  $\psi_1$ , is a constant and  $n_1$  and  $m_1$  are empirical exponent which typically depend on operating conditions, thermo-physical properties of the refrigerant and surface conditions. The equation (15) is proposed for predicting the boiling heat transfer coefficient of pure refrigerants for engineering applications. In dimensionless form, a correlation for plain and enhanced tube of the present boiling data was developed following Kutateladze [17] as :

$$Nu = \psi_2 Re^{n_2} K_p^{m_2} \tag{16}$$

In Eq. (16) the dimensionless groups are : Nusselt number  $Nu = \alpha x / k$ , Reynolds number  $Re = qx / \rho_v h_{fg} \nu$  and Kutateladze boiling number  $K_p = P / \sqrt{g \rho_l \sigma}$

According to Kutateladze [A], the reference length (x) for Nu and Re is taken proportional to bubble departure diameter as  $\sqrt{\sigma / g(\rho_l - \rho_v)}$ .

The values of  $\psi, n$  and  $m$ , for equations 15 and 16 for the test tubes and refrigerants are given in table 5 below:

Table 5. Values of constant  $\psi_i$  and exponents,  $n_i$  and  $m_i$  of Eqs 15 and 16

Tube	$\psi_1$		$n_1$		$m_1$		$\psi_2$		$n_2$		$m_2$	
	R12	R134a	R12	R134a	R12	R134a	R12	R134a	R12	R134a	R12	R134a
PT	0.015	0.027	0.7	0.67	0.8	0.82	0.73	0.96	0.66	0.65	0.73	0.73
RF	0.05	0.63	0.68	0.65	0.7	0.6	1.4	5.1	0.65	0.62	0.6	0.5
LF	2.3	17.7	0.6	0.5	0.41	0.34	9.2	13	0.6	0.46	0.36	0.33
SM	4.2	33.5	0.55	0.4	0.34	0.3	11.7	17.5	0.55	0.42	0.33	0.27

An inspection on the table 5, indicates that the values of exponents n, and m for the enhanced tubes are lower than those for plain tube. This means that the effect of the surface conditions is more dominant over the operating conditions (q and P). This statement is clearly appears for the case of SM tube, having the lowest values of n and m, which can be attributed to the increased nucleation sites density compared with other tested tubes as previously highlighted.

The equations 15 and 16 were derived using standard procedure of the least squares method for the range of effective variables of :

$$\begin{array}{rcl} 2.000 & \leq & q \leq 10000 \text{ W/m}^2 \\ 241 & \leq & P \leq 370 \text{ kPa.} \\ 0.8 & \leq & Re \leq 6 \\ 18 & \leq & Kp \leq 30 \end{array}$$

Figures 8a and 8b show the performance plots for Eqs 15 and 16, respectively. The correlations predict 95% of the data points within  $\pm 20\%$  which is satisfactory for the pool boiling calculations.

### CONCLUSIONS

An experimental data base has been established for pool boiling of pure R12 and R134a from single tubes drawing plain and enhanced surfaces. Based on the experimental data the following conclusions may be made.

1. All enhanced tubes perform better than the plain one at all conditions, exhibiting higher heat transfer coefficients. Enhancement ratios ranging from 1.1 to 2.9, times, for radial finned tube, 3 ~ 4.6 for longitudinal finned tube are resulted. At the same, time the enhancement becomes more significant with screen matrix tube and reaches about 5 times.
2. The trend of enhancement can be explained from consideration of various mechanisms of bubble formation and bubble dynamics, as well as nucleation sites density.
3. For all tested tubes at given saturation temperatures, the boiling coefficients of R134a are higher than those for R12. This is apparently due to the thermo-physical properties of R134a resulting higher boiling coefficient. The enhancement decreases, when the screen matrix is tested due to the dominant effect of surface condition over physical properties.
4. The screen matrix tube provides the largest enhancements up to 5 times compared with plain tube. This finding is of great use for flooded type evaporators.
5. Two correlations for the present boiling data was developed. This correlation satisfactory expresses the influences of the operating conditions on the boiling coefficient. The correlations can be used to predict the boiling coefficient with a reasonable accuracy.

### ACKNOWLEDGMENTS

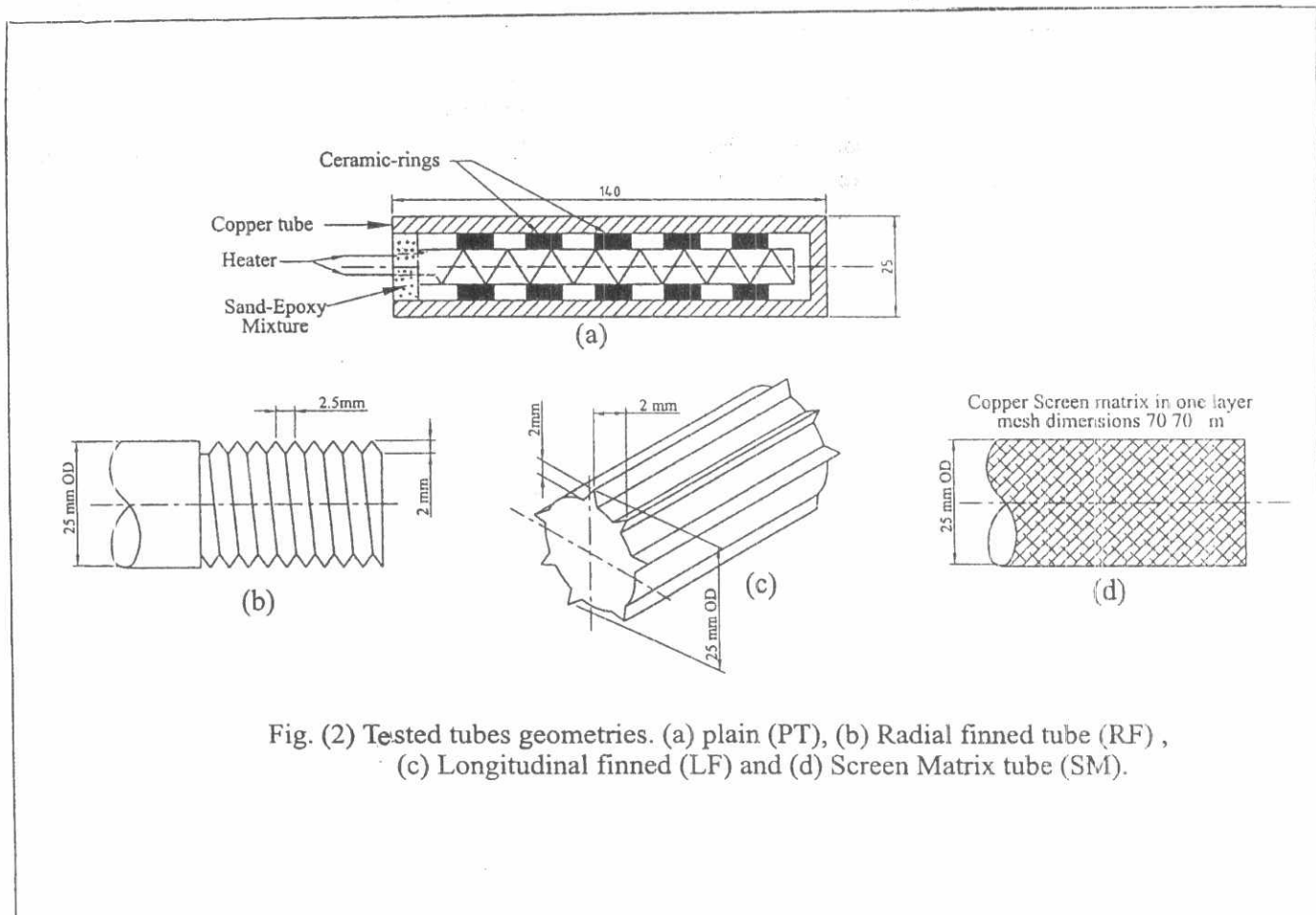
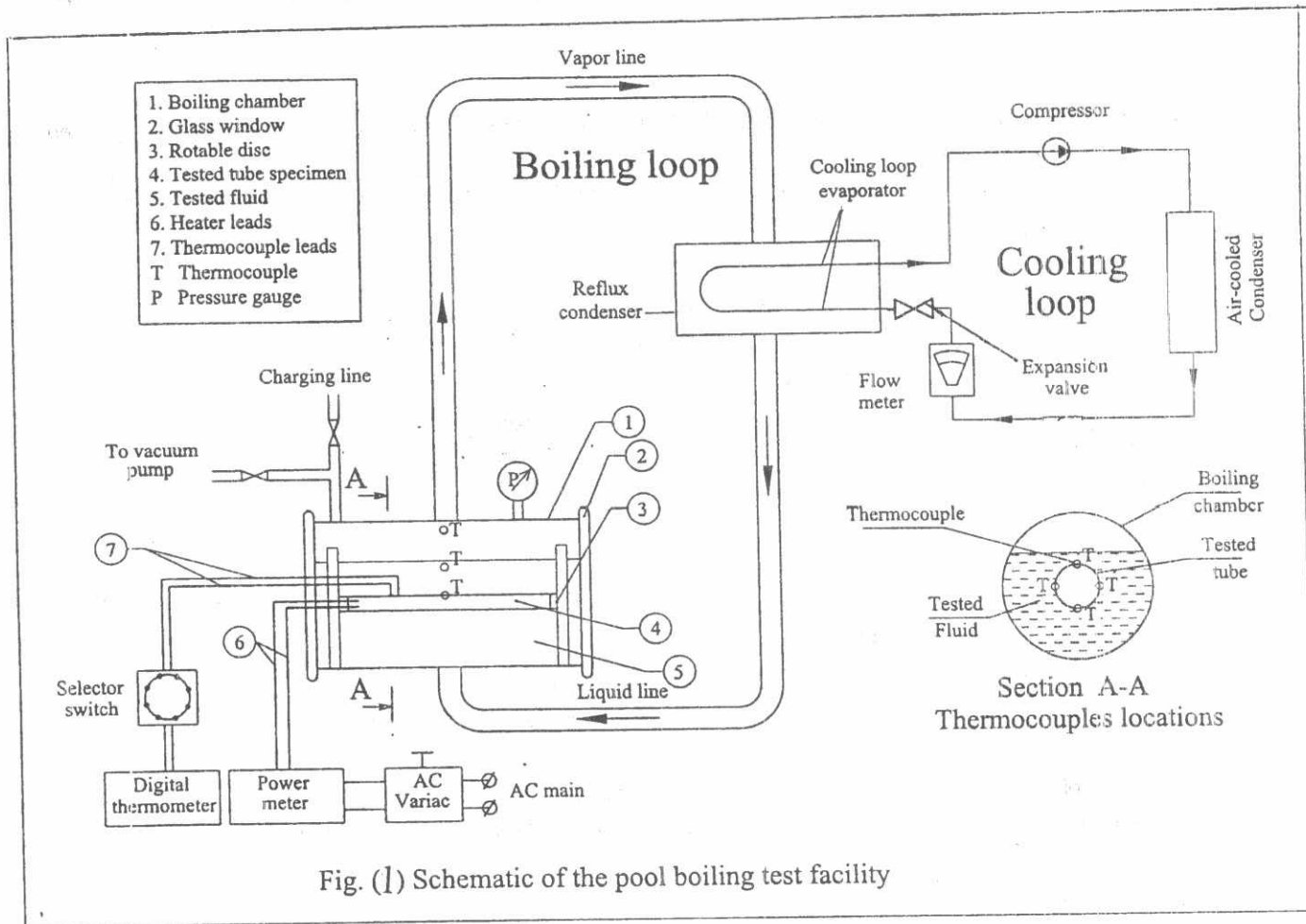
The authors would like to express their appreciation for Profs. M.A El Hefni, R.M. Abdel Wahid, and K.A. El Shorbagy for valuable suggestions and scientific aids.

### REFERENCES

1. I.G. Chomac, M.A. Aziz and V.P Gaverlkin "Raising the Efficiency of Refrigerant Evaporator"; Khold Technica, Vol 43 pp 10-14, 1986. (In Russian)
2. C. Pais and R.L Webb; "Literature Survey of Pool Boiling on Enhanced Surfaces"; ASHRAE transaction, Vol. 97 pp 79-89, 1994.
3. C.B. Chiou and D.C.Lu; "Pool Boiling of R22, R124 and R134a on a Plain Tube"; Int. J. Heat Mass Transfer, Vol 40 No. 7. pp 1657-1666, 1997.
4. S.S. Hsich and C.J. Weng; Nucleate Pool Boiling Heat Transfer Coefficients of Distilled Water (H<sub>2</sub> O) and R-134a/Oil Mixture From Rib-Roughered Surfaces"; ASME J of Heat Transfer, Vol 119, pp 142-151, 1997.
5. R.L. Webb and C. Pais; "Nucleate Pool Boiling Data for Five Refrigerants on Plain/Integral-Fin and Enhanced Tube Geometries"; Int. J. Heat Mass Transfer Vol 35 No. 8, pp 1893-1904, 1992.
6. R.L. Webb and C. Pais; "Pool Boiling for Five Refrigerants on Three Tube Geometries ASHRAE transactions Vol. 97 pp 72-78, 1991.
7. E.H Chen Qiu-Rong and R. Windisch; "Pool Boiling Heat Transfer on Finned Tubes An Experimental and Theoretical Study"; Int. J. Heat Mass Transfer, Vol 34 No. 8 pp 2071-2079, 1991.



8. J.Y. Change and S.M. You; "Boiling Heat Transfer Phenomena From Micro-Porous Surfaces in Saturated FC-72"; *Int. J. Heat Mass Transfer* Vol 40 No. 18, pp 4437-4447, 1997.
9. J.Y. Chang and S.M. You; "Enhanced Heat Transfer From Micro-Porous Surfaces: Effect of Coating Composition and Method *Int. J. Heat Mass transfer*, Vol 40, No 18, pp 4449-4460, 1997.
10. M.A. Aziz; "Investigation of Thermal Characteristics of Freon Shell and Tube Evaporators With Screen Matrix". Ph.d Thesis, Odessa 1981. (in Russian).
11. S.S. Hsieh and C.I. Weng; "Nucleate Pool Boiling From Coated Surfaces in Saturated R134a and R. 407c"; *Int J. Heat Mass Transfer* Vol, 40 No.3 pp 519-532, 1997.
12. C.C. Wang, W. Y. Shieh, Y.J. Change and C.Y. Yang "Nucleate Boiling Performance of R-22, R-123, R-134a, R 410A, R407C on Smooth and Enhanced Tubes"; *ASHRAE Transaction* Vol 104, Part 1B pp 1314-1320, 1998.
13. K. Stephan and M. Abdel Salam; "Heat Transfer Correlations for Natural Convection Boiling *Int. J. Heat Mass Transfer*, Vol 23, pp 73-87, 1980.
14. N.H. Afgan and La. A. Jovic; "Boiling Heat Transfer From Surface With Porous Layers" *Int. J. Heat Transfer* Vol. 28 No. 2 pp 415-422, 1985.
15. Y.A. Zeigarnik and N. H. Afgan; "Degenerated Boiling as a Way To Enhance Heat Transfer". *Proceeding of the International Conference of Energy Research and Development* pp 1053-1062, Kuwait 9-11 November, 1998.
16. J.P. Holman. "Heat Transfer"; Source Book, Seventh Edition McGraw Hill London, 1992.
17. S.S. Kutateladze; "Principles of Heat Transfer Theory. Source Book in Russian, Atom Press Moscow, 1979.
18. G.H. Danilova; The Effect of Nucleation Site Number on Nucleate Pool Boiling Heat Transfer"; *Engineering Physical J. Vol. XI-No.3* pp. 367-370. 1966. Moscow. (in Russian).
19. G. Kocamustafa Ogullari and M. Ishii; "Interfacial Area and Nucleation Sites Density in Boiling Systems"; *Int. J. Heat Mass Transfer*, Vol 26. No. 9. Pp 1377-1387, 1983.
20. S. R. Yang; "A Mathematical Model of the Pool Boiling Nucleation Site Density in Terms of Thermal Characteristics"; *Int. J. Heat Mass Transfer. Vol. 31 No. 6* pp 1127-1135, 1988.
21. H.C. Liang and R-L. Webb; "A Nucleate Boiling Model For Structured Enhanced Surfaces"; *Int. J. Heat Mass Transfer. Vol. 41. No 14*, pp 2183-2195, 1995.
22. *ASHRAE Hand Book Fundamental* New York, 1997.



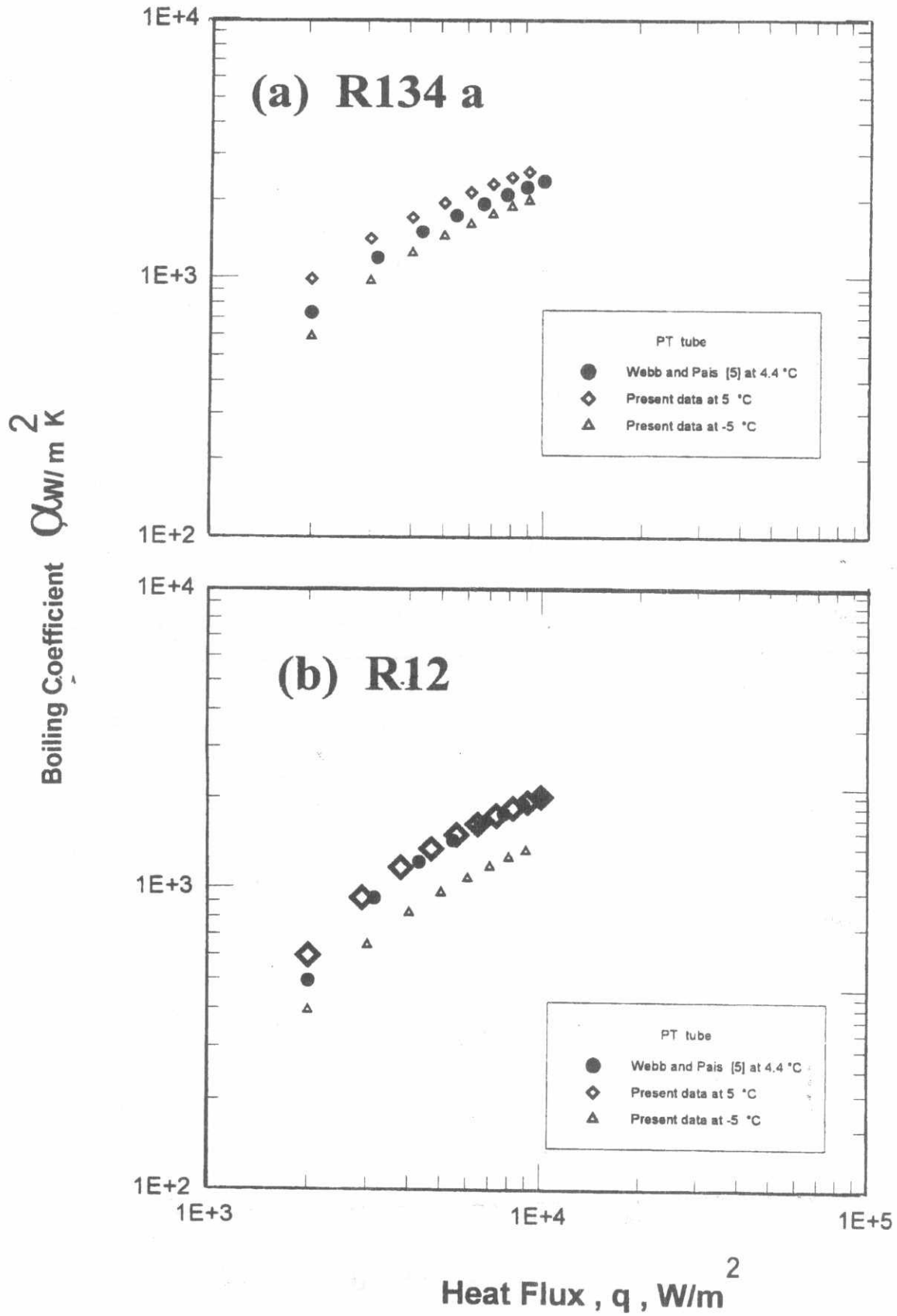


Figure 3 Present Boiling Curves of R12(a) and R134a (b) for Plain Tube. Compared with that of Webb and Pais [5]

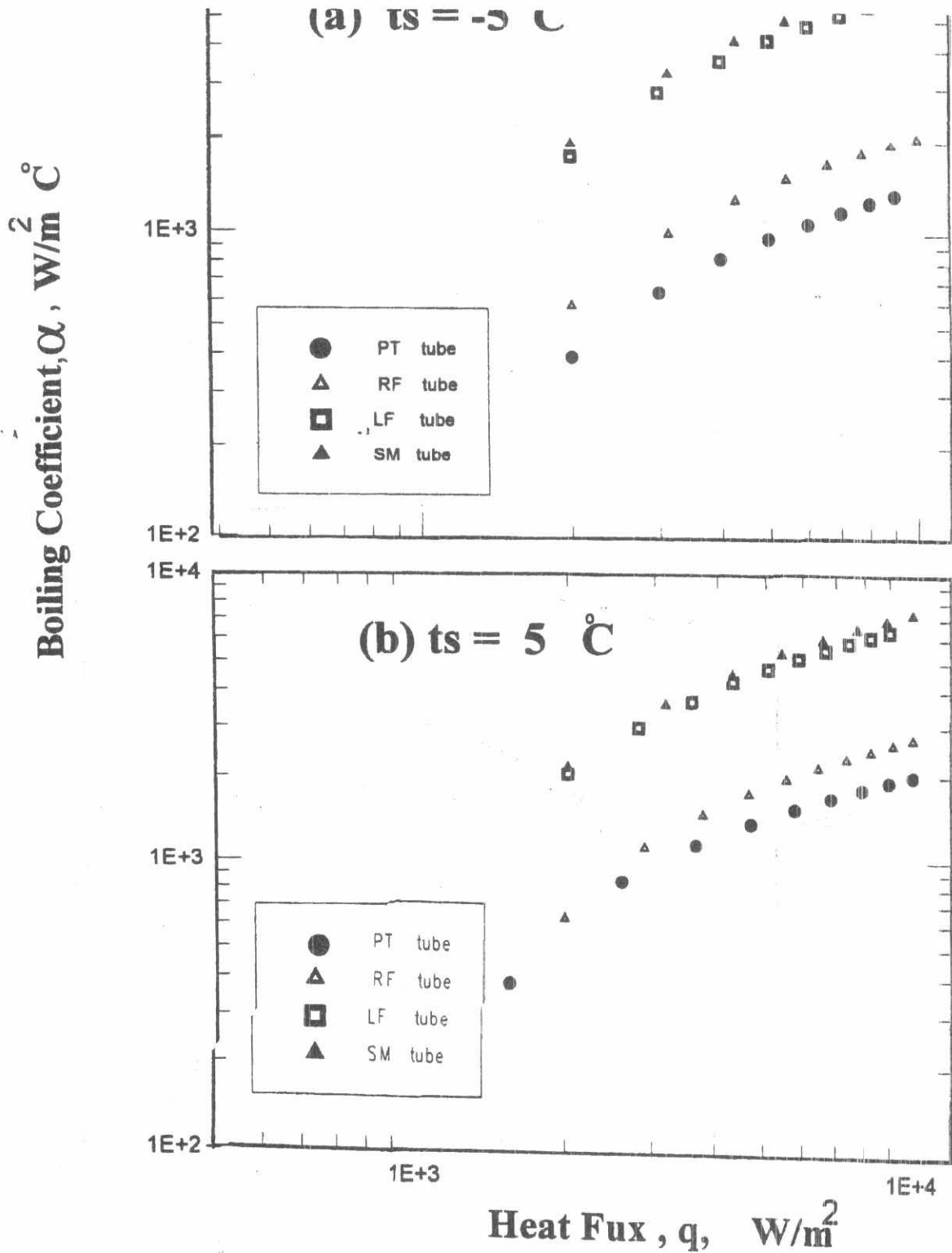


Figure (4). Boiling Curves of R12 for Plain and Enhanced tubes



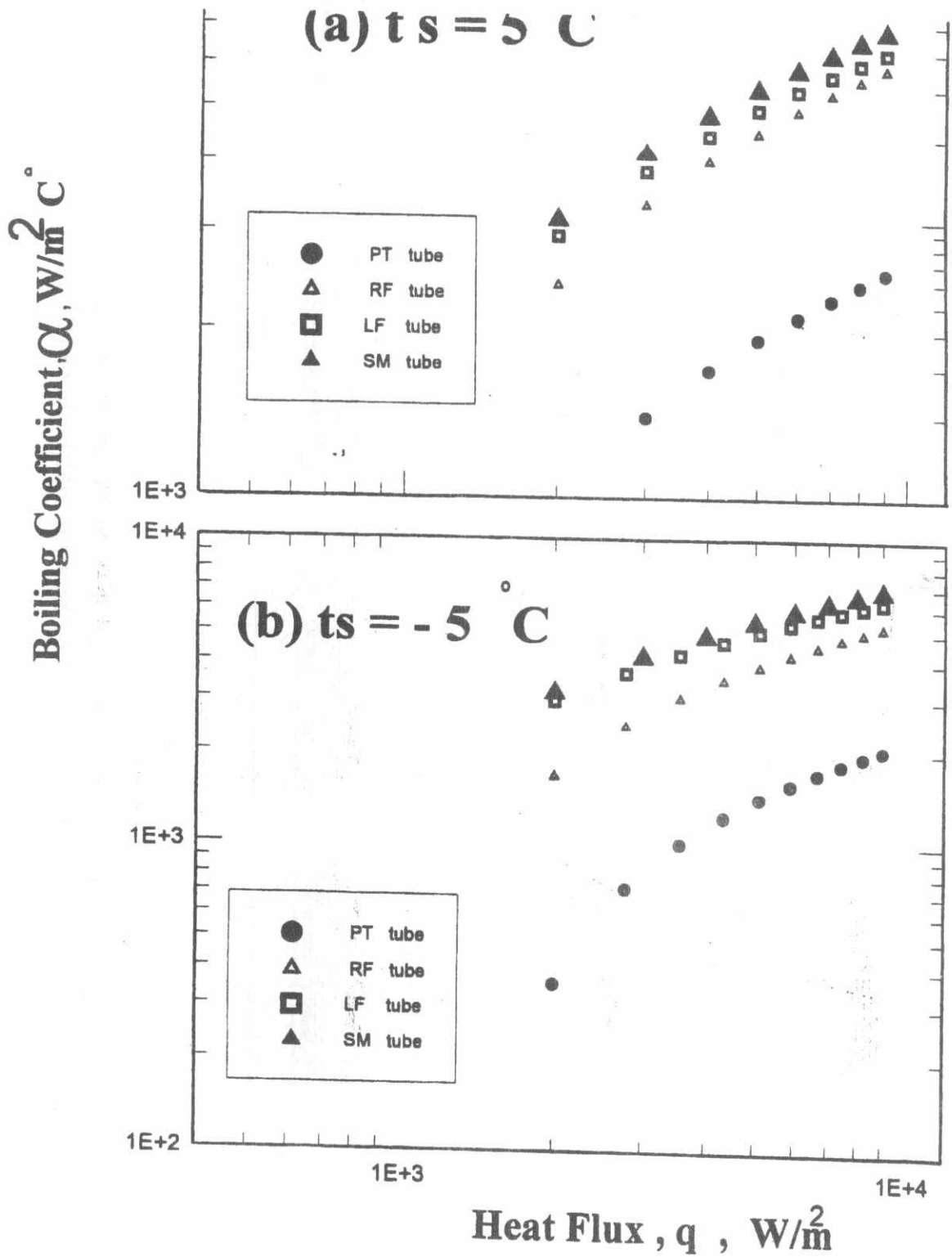


Figure (5). Boiling Curves of R134 for Plain and Enhanced tubes

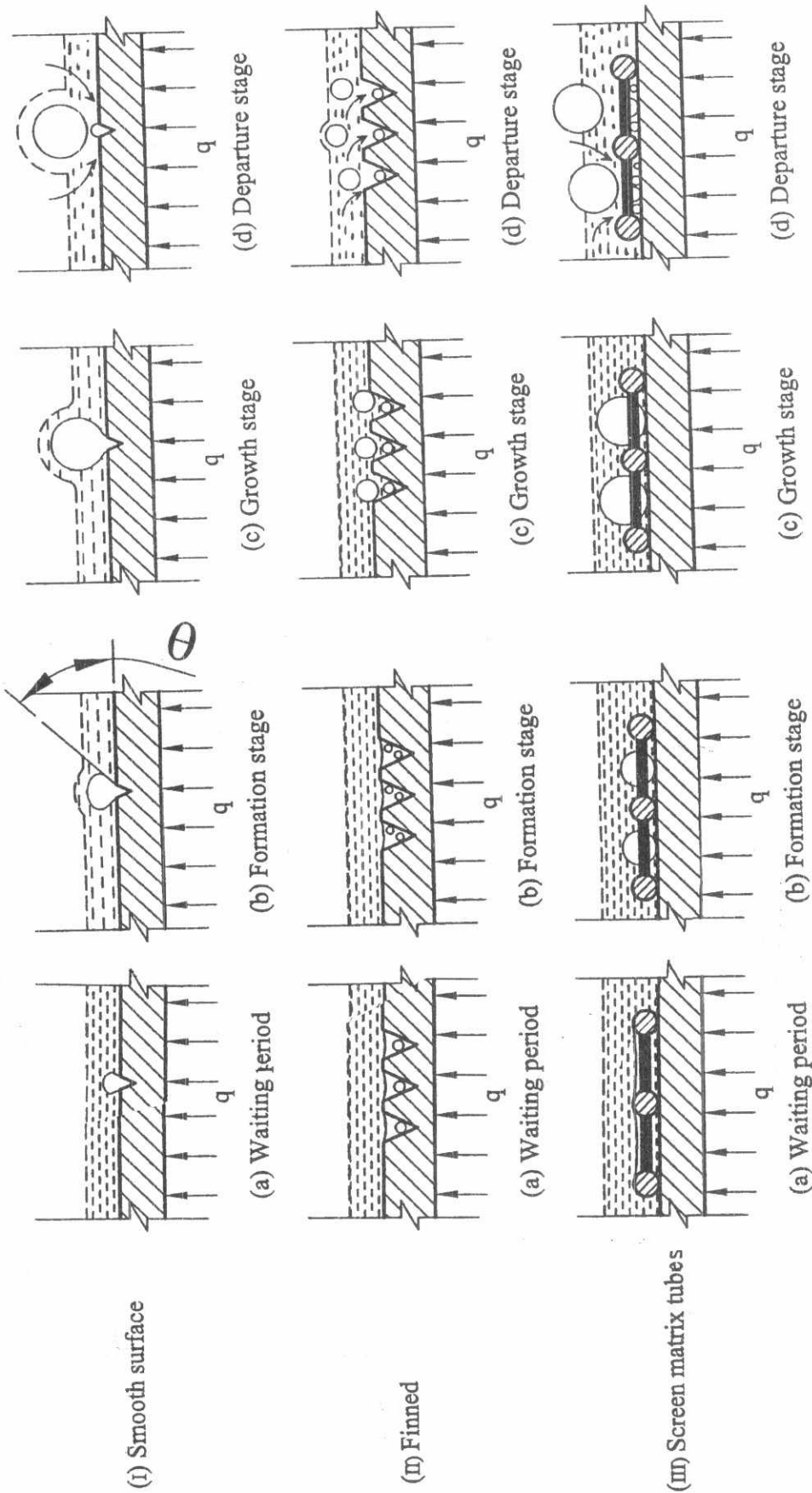
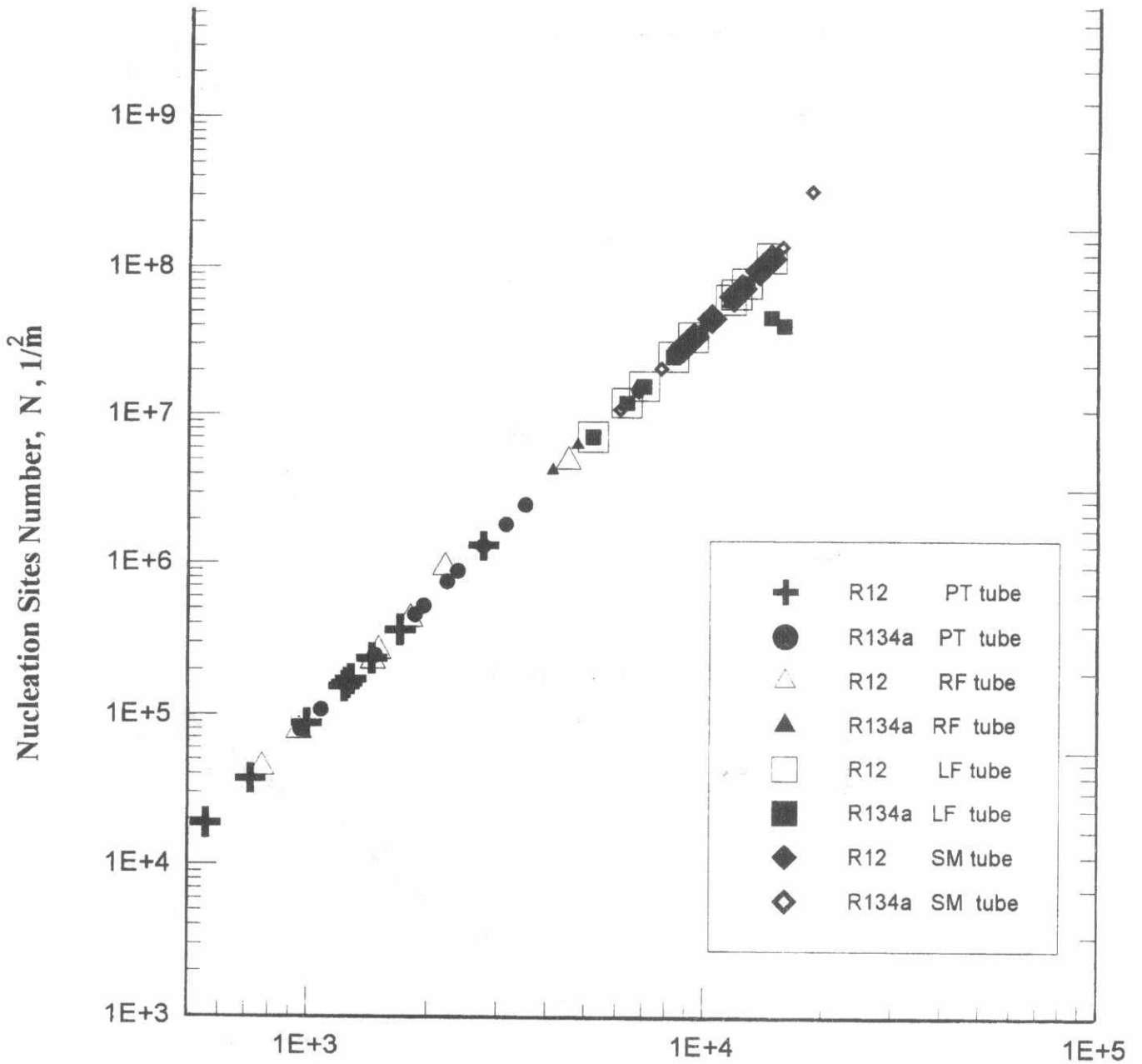


Fig. (6) Schematic of bubble formation on smooth (I), Finned (II), and Screen Matrix tubes. (III)



$$\frac{\alpha d_o^{0.25}}{K_1} \left( \frac{\rho_v h_{fg}}{\rho_l \cdot c_{pl} \cdot \Delta T_s} \right)^{0.5} \cdot Pr^{(0.39)}$$

Figure 7 Active Nucleation Sites Number  $N$  vs Heat Transfer Boiling Coefficient and Refrigerant Properties

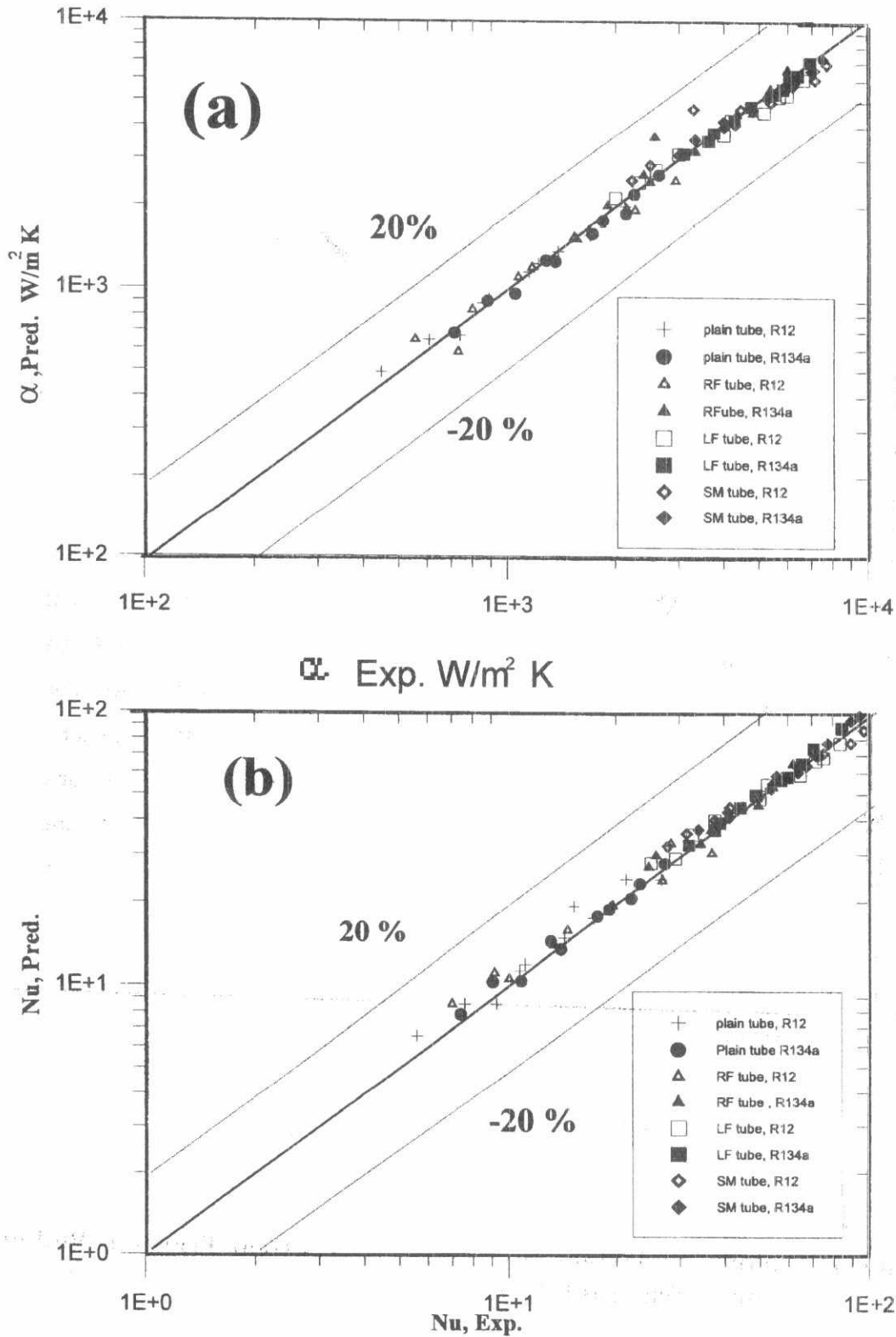


Figure (8) The present correlations and its deviation with expimental data  
 a- predicted by Eq. 15      b- Nu, predicted by Eq. 16